ISSN 1063-780X, Plasma Physics Reports, 2010, Vol. 36, No. 2, pp. 182–189. © Pleiades Publishing, Ltd., 2010.
Original Russian Text © Yu.A. Lebedev, T.B. Mavlyudov, V.A. Shakhatov, I.L. Epstein, M.A. Karpov, 2010, published in Fizika Plazmy, 2010, Vol. 36, No. 2, pp. 201–208.

LOW-TEMPERATURE PLASMA

Development of a Nonequilibrium Microwave Discharge at the End of a Cylindrical Electrode in Nitrogen at Reduced Pressures

Yu. A. Lebedev[a], T. B. Mavlyudov[a], V. A. Shakhatov[a], I. L. Epstein[a], and M. A. Karpov[b]

[a] *Topchiev Institute of Petrochemical Synthesis, Russian Academy of Sciences, Leninskiĭ pr. 29, Moscow, 119991 Russia*

[b] *Moscow State Institute of Radioengineering, Electronics, and Automation, pr. Vernadskogo 78, Moscow, 117454 Russia*

Received April 9, 2009; in final form, May 27, 2009

Abstract—Excitation of a microwave discharge at the end of a cylindrical electrode in nitrogen at a pressure of 1 Torr and incident powers of 60–140 W was investigated experimentally by using K-008 and K-011 video cameras and analyzing oscillograms of discharge emission. The times during which the discharge is established in the radial and axial directions are found to be on the order of 10^{-4} and 10^{-2} s, respectively. The results obtained are analyzed using one-dimensional simulations of a discharge in nitrogen in a quasistatic approximation. The kinetic scheme includes 50 processes involving electrons, ions, and excited molecules and atoms. The time evolution of the concentrations of molecular nitrogen in the $N_2(C^3\Pi_u)$ and $N_2(B^3\Pi_g)$ states, responsible for the recorded discharge emission, is compared with the experimental data.

DOI: 10.1134/S1063780X10020091

1. INTRODUCTION

In recent years, nonuniform electric discharges excited in a wide range of gas pressures and field frequencies have attracted considerable attention. Interest in such discharges is motivated, on the one hand, by the necessity of developing special technologies for creating quasi-uniform plasma systems, which is impossible without knowing the physics of nonuniform discharges. On the other hand, in order to find new fields of application of nonuniform discharges themselves, it is also necessary to know their properties. A specific type of nonuniform discharge is an electrode microwave discharge (EMD) excited at reduced pressures near a rode antenna placed in a large-size metal discharge chamber [1–3].

An efficient method for studying physical processes in gas discharges is to investigate relaxation phenomena occurring in them [4]. Here, we present the results of experimental studies of the time evolution of optical emission from an EMD in nitrogen in the course of discharge development. The results obtained are analyzed using a kinetic model of plasma processes.

2. EXPERIMENTAL SETUP, DIAGNSTIC TECHNIQUES, AND COMPUTATIONAL MODEL

2.1. Experiment

The experimental setup for generating an EMD and studying its properties was described in detail in [5]. It was, however, substantially modified as applied to the problems of the present study.

The discharge chamber was a 15-cm-diameter stainless-steel cylinder. The rode antenna (a 80-mm-long cylindrical copper tube with an outer diameter of 5 mm) was inserted into the discharge chamber through a vacuum-tight connection located in the upper part of the chamber. The EMD was ignited near the electrode end. The discharge was observed through the glass (VK-7) and quartz glass (KU-1) windows made in the side and bottom walls of the chamber.

A continuous electromagnetic wave with a power of up to 180 W and frequency of 2.45 GHz was input in the discharge chamber through a coaxial-to-waveguide converter, one component of which was the rode antenna. The waveguide line included elements for measuring the microwave power and standing-wave coefficient: a circulator, a measuring line, and a detector of the incident power P_{in}. The waveguide line was matched using a shirt-circuiting piston and a three-stub transformer. The microwave spectrum was measured using an S4-27 spectrum analyzer and an S7-11 stroboscopic oscilloscope. Time variations in the microwave parameters and integral plasma radiation were also measured using a Tektronix TDS2021B oscilloscope. In these experiments, the rode antenna and the discharge chamber were dc short-circuited and were at the same electric potential. The setup was equipped with AvaSpec-2048 (1-nm resolution) and

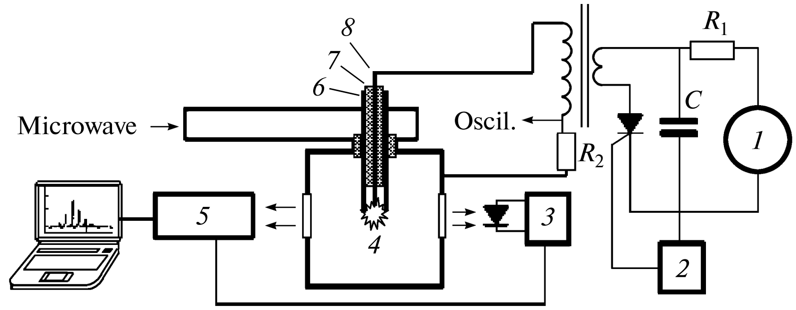

Fig. 1. Scheme of discharge ignition: (*1*) dc voltage source, (*2*) generator of the start-up signal, (*3*) generator of the synch pulse, (*4*) spark, (*5*) K-008 and K-011 video cameras, (*6*) rode antenna, (*7*) insulator, (*8*) igniting electrode, (*C*) storage capacitor (0.2 μF), (R_1) charging resistor (1 MΩ), and (R_2) measuring resistor (3 Ω).

AvaSpec-2048-4-RM (0.1-nm resolution) spectrometers operating in four spectral ranges.

The experiments were carried out in a nitrogen flow. The nitrogen flow rate was 1–200 sccm. In contrast to our previous studies, the gas was supplied through an aperture in the chamber cover, rather than through the electrode channel. Previous experiments have shown that, for such flow rates, the structure and properties of the EMD are independent of the method of gas supply. The gas pressure in the discharge chamber was varied in the range 1–15 Torr.

To study the transition from the ignition stage to a steady-state regime, the setup was additionally equipped with K-008 (one-frame) and K-011 (nine-frame) nanosecond electron optical video cameras. The operating spectral range of the cameras was 400–800 nm. The exposure time and interval between frames of the K-011 camera could be varied in the range 0.1–100 μs.

The arrangement of the experiments depended on the microwave field strength. To provide gas breakdown by a strong microwave field, it is required to use a pulsed microwave source synchronized with measuring devices. In our case, however, the microwave source power was too low to produce gas breakdown and was sufficient only to maintain a steady-state discharge.

We designed and manufactured a spark system for discharge ignition (Fig. 1). The spark gap—a high-voltage molybdenum electrode with quartz insulation—was located in the channel of the rode antenna. Its bare section was inside the channel and did not do beyond the end of the rode antenna, so it did not perturb the microwave field structure. Spark discharge occurred near the open end of the rode antenna, between the bare section of the high-voltage electrode and the inner surface of the antenna channel. The high-voltage pulse was generated by discharging a storage capacitor through the primary winding of a step-up transformer. The storage capacitor was charged to the minimum voltage required for discharge ignition. The system was triggered by a start-up pulse supplied to a thyristor in the circuit of the primary winding. The start-up pulse was formed by a special circuit, which could also generate a synch pulse for triggering the measuring system. However, in this series of experiments, to avoid errors in the start-up times of video cameras due to scatter in the ignition time, the synch pulse was produced by a photodiode reacting to the spark discharge. The inductance and parasitic capacitance of the ignition circuit formed transient oscillations damped over a time shorter than 500 ns.

The experiments were carried out as follows. First, the microwave source was switched on, but the microwave power was insufficient to excite a discharge. Then, the igniting pulse generated a spark, which triggered the video cameras recording the development of a spark-initiated microwave discharge with preset frame exposure times and intervals between frames.

2.2. Model

To qualitatively analyze some of the experimental results, we performed one-dimensional simulations of an EMD in nitrogen. The computational code was based on a simplified quasistatic model of a microwave discharge between two spherical electrodes. Previously, this model was used in [6–8] to simulate discharges in nitrogen and oxygen at reduced pressures and was demonstrated to be capable of adequately describing the general properties of the discharge. We modified this model to describe non-steady-state processes, in particular, the process of discharge ignition.

The model includes the equation for the electric field in the quasistatic approximation (the microwave electric field is assumed to be parallel to the plasma density gradient), time-dependent balance equations for charged (e, N^+, N_2^+, N_3^+, and N_4^+) and neutral ($N_2(A^3\Sigma_u^+)$, $N_2(B^3\Pi_g)$, $N_2(C^3\Pi_u)$, $N_2(a'^1\Sigma_u^-)$, $N(^4S)$, $N(^2D)$, and $N(^2P)$) plasma particles with allowance for particle diffusion and particle production and loss due to bulk recombination and chemical reactions, and Poisson's equation for the charge-separation field. The reactions taken into account in this model and the corresponding rate constants are given in [7]. The rate constants of reactions involving electrons were assumed to be functions of the local value of the microwave field and were calculated using the electron energy distribution function obtained by solving the time-independent homogeneous Boltzmann equation [9]. In solving this equation, we used a set of cross sections for nitrogen kindly put in our disposal by I.V. Kochetov. The diffusion coefficients for all neutral excited plasma components were assumed to be equal to the diffusion coefficients of the corresponding particles in the ground state. The effect of vibrationally excited nitrogen molecules on plasma processes was taken into account by applying a simplified approach based on the analytic expression for the distribution function of molecules over vibrational states obtained in the diffusion approximation in [10].

2.2.1. Initial and boundary conditions. At the initial instant, the densities of all particles, except for electrons and N_2^+ ions, were assumed to be zero. The electron density profile was specified as a narrow (a few-millimeters-wide) parabolic function. The maximum electron density n_{max} was two to three times higher than the critical density ($n_c = 7.44 \times 10^{10}\,cm^{-3}$). The initial N_2^+ density was assumed to be equal to the electron density. The width of the initial plasma density profile and the maximum electron density were varied. At times on the order of 10^{-7} s and longer, the simulation results did not depend on the initial distribution of the electron density. To test the sensitivity of the simulation results to the initial conditions, we also performed simulations with a nonzero initial density of $N_2(A^3\Sigma_u^+)$ (see Section 3).

The densities of charged particles at the electrodes were assumed to be zero. The potentials of both electrodes were set at zero. The densities of nitrogen atoms and molecules in the ground state at the electrodes were determined from the equations

$$D_N\frac{dn_N}{dr} = \pm\frac{1}{4}\gamma v_t n_N, \quad D_{N_2}\frac{dn_{N_2}}{dr} = \mp\frac{1}{8}\gamma v_t n_N,$$

where γ is the recombination probability of nitrogen atoms on the walls, $\gamma = 10^{-4}$–10^{-3}, and v_t is the thermal velocity. For all other neutral particles, the electrode surface was assumed to be perfectly catalytic, so their densities at the electrodes were assumed to be zero.

2.2.2. Numerical algorithm. The time-dependent continuity equations for all particles were solved numerically by using an implicit scheme. To solve the continuity equations for electrons and positive ions, as well as Poisson's equation, we used the algorithm proposed in [11, 12], in which charged particle flows were approximated using the Sharfetter and Gummel exponential scheme [13]. The obtained set of nonlinear equations was solved by Newton's method.

The problem was solved on a uniform mesh with the number of cells from 100 to 600.

3. RESULTS AND DISCUSSION

The objective of this study was to investigate the transition from spark ignition to a steady-state discharge mode. In view of uncertainties in the times at which the discharge was photographed, the intervals between frames were chosen so as to obtain a series of images characterizing the entire transition process. The frame exposures were the same (1 μs); therefore, the image brightness corresponds to the actual intensity of discharge radiation. The first frame corresponds to the instant of spark ignition. The discharge is initiated at the end of the vertically oriented electrode. The results of measurement carried out at a pressure of 1 Torr and different incident microwave powers are illustrated in Fig. 2. Taking into account the spectral sensitivity of the electron optical cameras, it could be expected that the discharge images are mainly produced by the 500- to 800-nm radiation of the first positive system of nitrogen ($N_2(B^3\Pi_g \to A^3\Sigma_u^+)$. This is confirmed by the fact that the image brightness remained practically unchanged when the discharge was photographed through a UV filter. The structure of a steady-state discharge is shown in Fig. 3. The signal from a microwave detector installed in the waveguide and the time evolution of the integral intensity of discharge radiation (the discharge radiation was focused onto the photodiode receiving surface) in the course of discharge ignition are shown in Fig. 4.

It is seen that, in any stage, the EMD consists of a bright electrode sheath and a spherical region, the dimensions of which depend on the incident microwave power. A comparison of photographs obtained in the transition stage (Fig. 2) and steady-state mode (Fig. 3) shows that the diameter of the spherical region reaches its steady-state value over a time on the order of 10^{-4} s. This time remains practically unchanged as the incident power varies from 60 to 140 W. It is this time that will be compared below with the simulation results.

It can be seen from the microwave detector signal (Fig. 4) that a steady-state structure of the microwave field is established over a time less than 1 ms. On the other hand, two characteristic segments can be distinguished in the photodetector signal (Fig. 4). The radiation intensity increases abruptly over a fraction of a millisecond, while the time during which it reaches its steady-state value is on the order of 10 ms. The difference in the results presented in Figs. 2 and 4 can be explained as follows. When measuring the EMD radiation focused onto the radiation detector, the main contribution to the recorded signal is made by the electrode sheath, in which up to 90% of the deposited

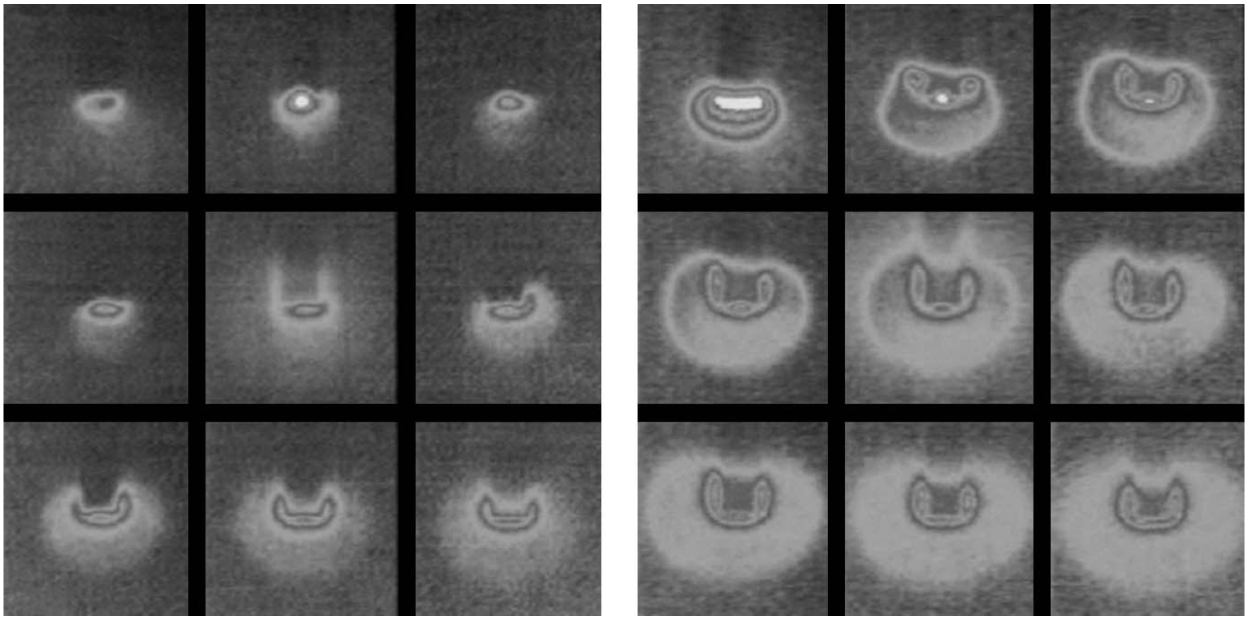

Fig. 2. Series of photographs illustrating the development of an EMD in nitrogen at a pressure of 1 Torr and incident microwave powers of 60 and 140 W. The frame exposure is 1 μs, and the time intervals between successive frames are 2, 5, 5, 5, 25, 50, 100, and 100 μs, respectively. The photographs were taken using the K-011 camera.

energy is concentrated [1–3]. Thus, the curve in Fig. 4 characterizes the time evolution of the total intensity of the electrode region. The K-011 camera is capable of recording discharge images at the times no longer than several milliseconds. The maximum recording time is reached at a maximum frame duration and maximum time intervals between frames (100 μs); in this case, however, information on the initial stage of the discharge is lost. To clarify the situation, let us compare Figs. 2 and 3. It is seen that, in the steady state (Fig. 3), the length of the electrode sheath covering the antenna is greater than that in the transition stage (Fig. 2). This means that, in the stage corresponding to the maximum time in Fig. 2, the discharge has not yet formed completely. It is also seen from the figures that, in the transition stage, the discharge has the shape of an ellipsoid, whereas in the steady state, it has the shape of a sphere with nearly the same diameter.

The electrode sheath begins to develop from the electrode center, where the spark discharger is located. Then, it propagates over the electrode end and moves up along the electrode toward the microwave source. This process is rather slow and seems to be related to gas heating and gas motion along the electrode. Note, that gas-dynamic effects in an EMD were previously observed when studying the spatial distributions of the gas temperature in hydrogen and nitrogen. The gas temperature was shown to be constant along the discharge radius due to vortex gas motion [14].

It follows from the above experimental results that the system is two-dimensional and that its characteristic formation times along and perpendicular to the discharge axis are different. These times are determined by different physical processes. This means that correct analysis of the process of discharge formation requires applying two-dimensional models that should take into account gas heating and gas dynamics. The one-dimensional model used in the present study can only be used to qualitatively describe discharge development in the radial direction.

It is worth noting a specific feature of the applied method of discharge initiation that should be taken into account when analyzing the results obtained. Photographs of the discharge at a zero incident microwave power show that, although the discharge process in the ignition circuit is completed over a time less than 500 ns (less than the exposure time of the first frame), the ignition afterglow is observed during 10 μs. This means that the first stage of the microwave discharge takes place in the active medium formed by the spark. Thus, the actual initial stage of the EMD may be shorter than that without residual phenomena of the spark discharge. These times, however, are significantly shorter than the total time during which the discharge reaches a steady state, so the latter time remains unperturbed. This is indirectly confirmed by the experimental fact that this time is independent of the spark discharger voltage, on which the densities of all particles produced in the spark should depend.

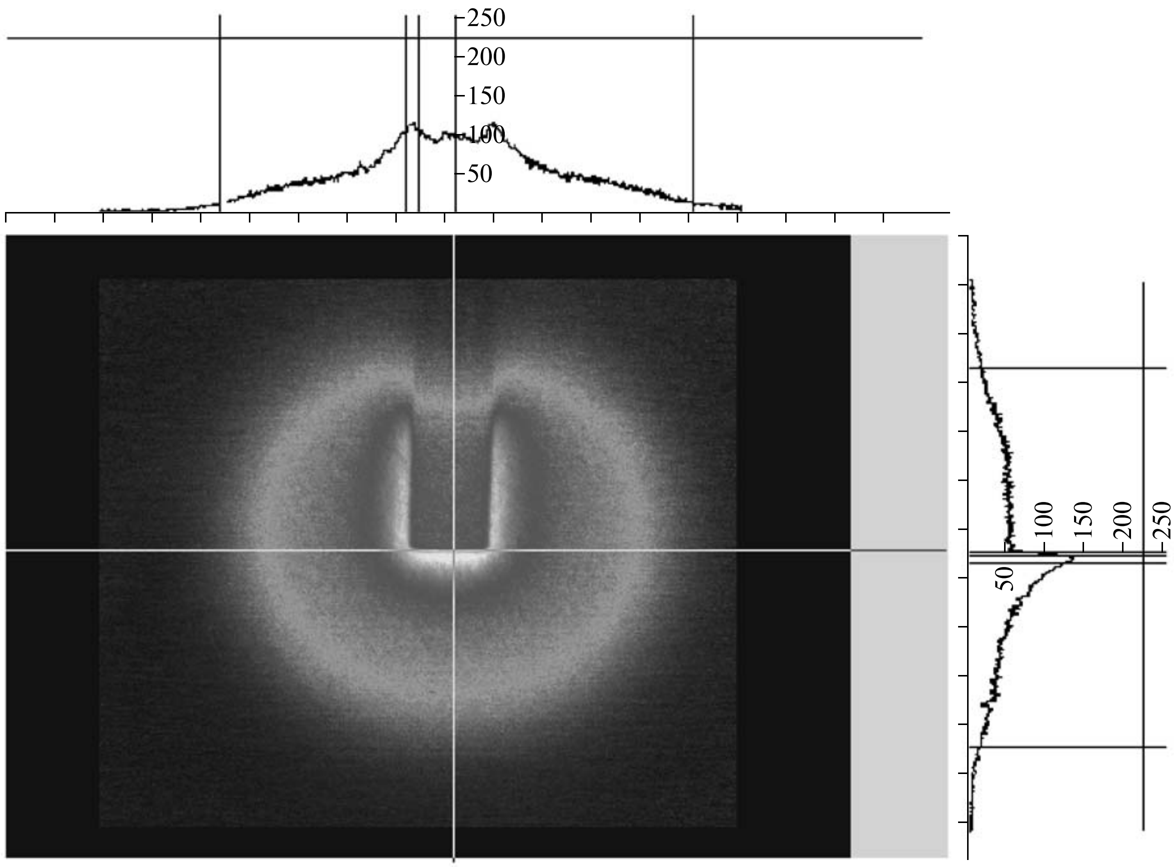

Fig. 3. Structure of a steady-state EMD in nitrogen at a pressure of 1 Torr and an incident microwave power of 120 W. The curves show the spatial distribution of the integral intensity of discharge radiation in the radial (the upper plot) and axial (the lower plot) cross sections (the cross sections on the photograph are shown by straight lines). The diameter of the electrode in the center of the photograph is 5 mm. The photograph was taken using the K-008 camera.

The main component of such an active medium may be the molecular nitrogen state $N_2(A^3\Sigma_u^+)$, which significantly affects the processes of excitation and ionization in plasma [7]. To study the effect of this state on the development of an EMD, we perform two series of one-dimensional simulations. In the first series, only the initial electron density was preset, whereas in the second series, the initial densities of electrons and molecules in the $N_2(A^3\Sigma_u^+)$ state were specified. Our simulations showed that, at times of 10^{-4} and 10^{-3} s, the results obtained were almost the same. Therefore, further simulations were performed over the time 10^{-4} s and the initial density of nitrogen molecules in the $N_2(A^3\Sigma_u^+)$ state was set at zero. Typical simulation results are presented in Figs. 5–7. Since the discharge plasma exists only near the central electrode, the figures show only this region and the radial coordinate is not continued up to the outer electrode.

The simulation results can be briefly formulated as follows. The value and time dependence of the microwave field strength (Fig. 5a), as well as the densities of electrons (Fig. 5b) and nitrogen molecules in the $N_2(C^3\Pi_u)$ state (Fig. 6b), which is responsible for the radiation of the second positive system of nitrogen (the $N_2(C^3\Pi_u \to B^3\Pi_g)$ transition), do not change when the initial density of nitrogen molecules in the $N_2(A^3\Sigma_u^+)$ state is set at zero. This means that the $N_2(C^3\Pi_u)$ state is mainly excited by electron impact $(N_2(X^1\Sigma_g^+) + e \Rightarrow N_2(C^3\Pi_u) + e)$, whereas the contribution of associative excitation $(N_2(A^3\Sigma_u^+) + N_2(A^3\Sigma_u^+) \Rightarrow N_2(C^3\Pi_u) + N_2)$ plays a minor role (see also [12], [19]). Therefore, the density of molecules in the $N_2(C^3\Pi_u)$ state in the electrode region is established almost instantaneously and the expansion of the spherical discharge region where molecules in this state exist is caused by the diffusive expansion of the particles involved in the ionization process. Remember that the second positive system of nitrogen (the $N_2(C^3\Pi_u \to B^3\Pi_g)$ transition) predomi-

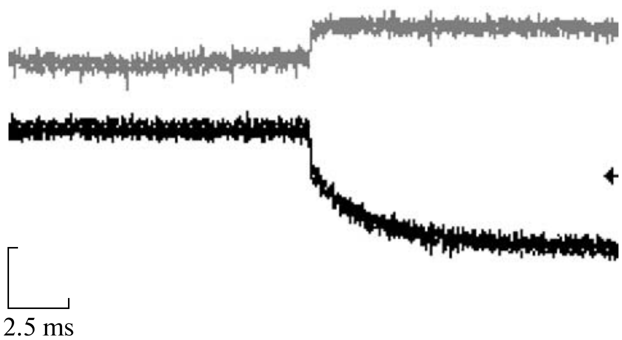

Fig. 4. Signal from the microwave detector installed in the waveguide (the upper curve) and time evolution of the integral radiation intensity (the lower curve) during the ignition of an EMD in nitrogen at a pressure of 1 Torr and an incident power of 90 W.

nates over other bands in the radiation emitted from the electrode region [14].

The presence of molecules in the $N_2(A^3\Sigma_u^+)$ state at the initial instant significantly affects the initial time evolution of the density of $N_2(B^3\Pi_g)$ molecules. In all stages, $N_2(B^3\Pi_g)$ molecules are produced via the reaction $N_2\left(A^3\Sigma_u^+\right) + N_2\left(A^3\Sigma_u^+\right) \Rightarrow N_2(B^3\Pi_g) + N_2$. For a zero initial density of $N_2(A^3\Sigma_u^+)$, while its amount produced via the reaction $N_2\left(X^1\Sigma_g^+\right) + e \Rightarrow N_2\left(A^3\Sigma_u^+\right) + e$ is small, the main channel for $N_2(B^3\Pi_g)$ production is electron excitation from the ground state $N_2\left(X^1\Sigma_g^+\right) + e \Rightarrow N_2\left(B^3\Pi_g\right) + e$. This is confirmed by an increase in the density of this state in the plasma resonance region. In the final stage of discharge development, molecular excitation is mainly determined by the process $N_2\left(A^3\Sigma_u^+\right) + N_2\left(A^3\Sigma_u^+\right) \Rightarrow N_2(B^3\Pi_g) + N_2$.

It should be noted that the calculated time during which the discharge reaches its steady state is on the order of 10^{-4} s and does not depend on the presence of $N_2(A^3\Sigma_u^+)$ molecules at the initial instant. The densities of all other plasma particles (including $N_2(A^3\Sigma_u^+)$) at a time of 10^{-4} s are also independent of the initial density of these molecules. In our experiments, this time corresponds to the instant at which the size of the spherical region reaches its steady-state value in the direction perpendicular to the discharge axis. Radiation from the spherical region is dominated by the first positive system of nitrogen, which is determined by the $N_2(B^3\Pi_g)$ state.

Thus, the igniting spark discharge perturbs the initial stage of an EMD, but does not affect the total time

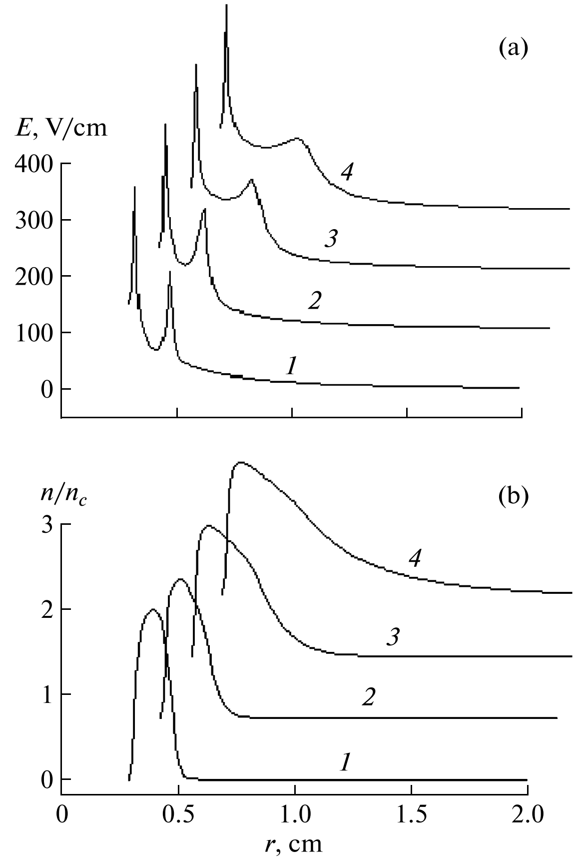

Fig. 5. Radial profiles of the (a) microwave field strength and (b) electron density for t = (*1*) 10^{-7}, (*2*) 10^{-6}, (*3*) 10^{-5}, and (*4*) 10^{-4} s.

during which the EMD reaches its steady state in the radial direction. Both the experimental data and simulation results show that this time is also independent of the incident microwave power.

We note once again that, in order to adequately describe the process of EMD formation, it is necessary to solve a two-dimensional time-dependent problem with allowance for gas heating and gas dynamics.

Our simulations have also shown that, at the instant of ignition, two space-charge layers form in the plasma resonance regions (Fig. 5a), where the electron density is equal to the critical one. One layer forms near the central electrode and is adjacent to the space-charge sheath similar to that existing near the surface of any body immersed in plasma. The second layer is located at the outer side of the descending density profile. As the radial profile of the electron density widens, the second layer expands and shifts toward the outer electrode and the electric field in it decreases from a few hundred to several units of V/cm. In a steady-state EMD, quasineutrality is violated and the space-charge layers exist near the electrodes and in the plasma resonance region at the outer boundary of the

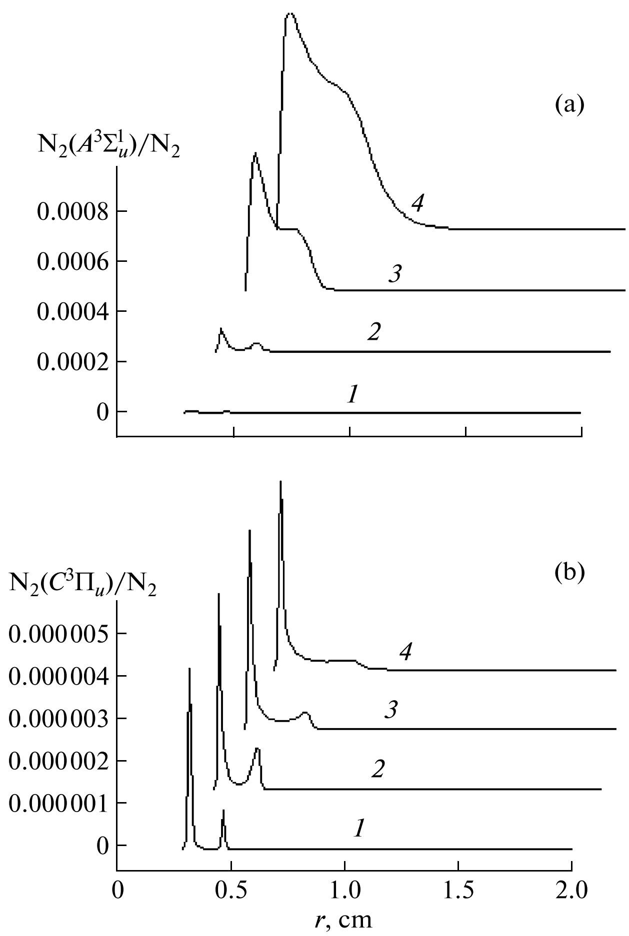

Fig. 6. Radial profiles of the densities of (a) $N_2(A^3\Sigma_u^+)$ and (b) $N_2(C^3\Pi_u)$ molecules for the same instants as in Fig. 5.

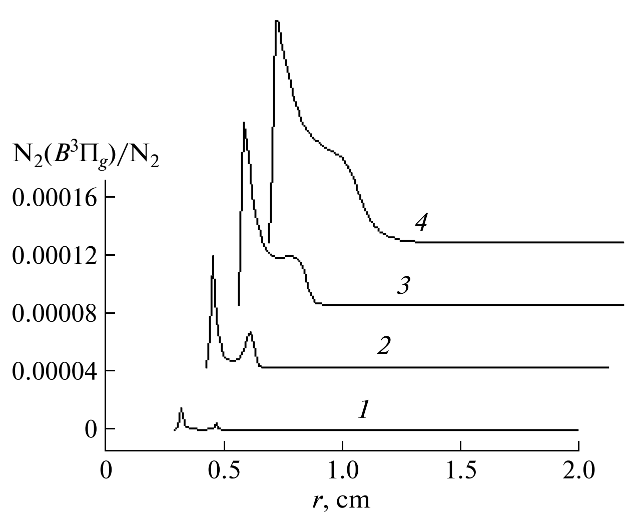

Fig. 7. Radial profiles of the density of $N_2(B^3\Pi_g)$ molecules for the same instants as in Fig. 5.

spherical region. Note, that the steady-state distribution of the space-charge field is established over a time on the order of several milliseconds, which is required for the plasma to fill the entire discharge chamber. Violation of plasma quasineutrality in the plasma resonance region was considered in detail in [15].

4. CONCLUSIONS

Our study of the development of an EMD in nitrogen at a pressure of 1 Torr has shown that, when the discharge is ignited at the electrode end, a steady-state discharge structure develops in the radial direction over a diffusion time on the order of 10^{-4} s and in the axial direction over a time on the order of 10^{-2} s, which is determined by gas heating and gas motion along the electrode. The parameters of the igniting spark discharge do not affect the time of EMD formation. The processes occurring during the development of the discharge can be divided into two groups: electron-impact processes and processes related to secondary phenomena. The first group includes excitation of the $N_2(C^3\Pi_u)$ emitting state, whereas the second group includes excitation of the $N_2(B^3\Pi_g)$ emitting state. This explains the difference in the formation times of different discharge regions. The $N_2(C^3\Pi_u)$ state is responsible for radiation from the region adjacent to the rode antenna (the second positive system of nitrogen). The observed formation time of the spherical discharge region is determined by the $N_2(B^3\Pi_g)$ state (the first positive system of nitrogen). The excitation reaction of this state involves $N_2(A^3\Sigma_u^+)$ molecules. Our results confirm the previous conclusion that, in a strongly nonuniform discharge, in particular, an EMD, there are regions with very different properties.

ACKNOWLEDGMENTS

This study was supported in part by the Russian Foundation for Basic Research, project no. 07-08-00020.

REFERENCES

1. Yu. A. Lebedev, in *Encyclopedia of Low-Temperature Plasma,* Vol. VIII-1: *Chemistry of Low-Temperature Plasma*, Ed. by Yu. A. Lebedev, N. A. Platé, and V. E. Fortov (Yanus-K, Moscow, 2005) [in Russian].
2. Yu. A. Lebedev, V. A. Shakhatov, A.V. Tatarinov, and I. L. Epstein, J. Phys., Conf. Ser. **44**, 30 (2006).
3. Yu. A. Lebedev, M. V. Mokeev, P. V. Solomakhin, et al., J. Phys. D **41**, 194 001 (1940).
4. D. I. Slovetskii, *Mechanisms of Chemical Reactions in Nonequilibrium Plasmas* (Nauka, Moscow, 1980) [in Russian].

5. Yu. A. Lebedev, P. V. Solomakhin, and V. A. Shakhatov, Fiz. Plazmy **34**, 614 (2008) [Plasma Phys. Rep. **34**, 562 (2008)].

6. Yu. A. Lebedev, A. V. Tatarinov, and I. L. Epstein, Teplofiz. Vys. Temp. **45**, 325 (2007).

7. Yu. A. Lebedev and I. L. Epstein, Fiz. Plazmy **33**, 68 (2007) [Plasma Phys. Rep. **33**, 63 (2007)].

8. Yu. A. Lebedev, A. V. Tatarinov, and I. L. Epstein, Teplofiz. Vys. Temp. **46**, 645 (2008).

9. Yu. A. Lebedev and I. L. Epstein, J. Moscow Phys. Soc. **5** (1) 103 (1995).

10. M. Capitelli, C. M. Ferreira, B. F. Gordiets, and A. I. Osipov, *Plasma Kinetics in Atmospheric Gases* (Springer-Verlag, Berlin, 2000).

11. J. Boeuf, J. Appl. Phys. **63**, 1342 (1988).

12. A. Fiala, L. Pitchford, and J. Boeuf, Phys. Rev. E **49**, 5607 (1994).

13. D. Sharfetter and H. Gummel, IEEE Trans. Electron. Dev. **16**, 64 (1969).

14. Yu. A. Lebedev, P. V. Solomakhin, and V. A. Shakhatov, Fiz. Plazmy **33**, 180 (2007) [Plasma Phys. Rep. **33**, 157 (2007)].

15. Yu. A. Lebedev, A.V. Tatarinov, and I. L. Epstein, Eur. J. Phys. D **53**, 319 (2009).

Translated by L.L. Borodina